

Rosiglitazone Induces Decreases in Bone Mass and Strength that Are Reminiscent of Aged Bone

Oxana P. Lazarenko, Sylwia O. Rzonca, William R. Hogue, Frances L. Swain, Larry J. Suva, and Beata Lecka-Czernik

Department of Geriatrics (O.P.L., S.O.R., B.L.-C.), Reynolds Institute on Aging, and Department of Orthopaedic Surgery (W.R.H., F.L.S., L.J.S.), Center for Orthopaedic Research, Barton Research Institute, University of Arkansas for Medical Sciences, Little Rock, Arkansas 72205

Peroxisome proliferator-activated receptor- γ (PPAR γ) regulates both glucose metabolism and bone mass. Recent evidence suggests that the therapeutic modulation of PPAR γ activity with antidiabetic thiazolidinediones elicits unwanted effects on bone. In this study, the effects of rosiglitazone on the skeleton of growing (1 month), adult (6 month), and aged (24 month) C57BL/6 mice were determined. Aging was identified as a confounding factor for rosiglitazone-induced bone loss that correlated with the increased expression of PPAR γ in bone marrow mesenchymal stem cells. The bone of young growing mice was least affected, although a significant decrease in bone formation rate was noted. In both adult and aged animals, bone volume was significantly decreased by

rosiglitazone. In adult animals, bone loss correlated with attenuated bone formation, whereas in aged animals, bone loss was associated with increased osteoclastogenesis, mediated by increased receptor activator of nuclear factor- κ B ligand (RANKL) expression. PPAR γ activation led to changes in marrow structure and function such as a decrease in osteoblast number, an increase in marrow fat cells, an increase in osteoclast number, and a loss of the multipotential character of marrow mesenchymal stem cells. In conclusion, rosiglitazone induces changes in bone reminiscent of aged bone and appears to induce bone loss by altering the phenotype of marrow mesenchymal stem cells. (*Endocrinology* 148: 2669–2680, 2007)

OSTEOPOROSIS, OBESITY, AND diabetes are major public health concerns because of their prevalence in our increasingly sedentary and aging society (1). The peroxisome proliferator-activated receptor- γ (PPAR γ) is a DNA-binding nuclear hormone receptor that has been shown to regulate bone mass, energy expenditure, and glucose metabolism (2–4). At the cellular level, diverse pathologies such as obesity and osteoporosis share several features including a genetic predisposition and a common cell progenitor (5).

With aging, bone loss occurs universally in animals and humans and, in contrast to postmenopausal bone loss, affects individuals regardless of their sex steroid status (6). Age-related bone loss occurs only at the endosteal surface, which is in contact with the bone marrow, and results from attenuated and unbalanced bone turnover as a consequence of an oversupply of osteoclastic cells relative to the need for bone resorption and an undersupply of osteoblastic cells relative to the need for cavity repair (6). Although aging has a negative effect on bone formation and osteoblast production, it has a positive effect on the proportion of fatty marrow and the number of marrow adipocytes (7). In humans, the fem-

oral cavity becomes occupied by fat by the third decade of life (7). Similarly, high fat content in the vertebral marrow is positively correlated with osteopenia and osteoporosis in both elderly men and postmenopausal women (5).

Osteoblasts and adipocytes share a common progenitor and are derived from marrow mesenchymal stem cells (MSC) (8). MSC commitment toward the osteoblast or adipocyte lineage occurs via a stochastic mechanism, in which lineage-specific transcription factors, such as runt-related transcription factor 2 (Runx2) for osteoblasts and PPAR γ 2 for adipocytes, are activated (9, 10). Aging alters the balance in lineage commitment of marrow MSC and increases their differentiation toward the adipocyte lineage while decreasing differentiation toward the osteoblast lineage (9, 11). These lineage changes are reflected in the expression pattern of phenotype-specific transcription factors: an increase in the expression of PPAR γ 2 and a simultaneous decrease in the expression of Runx2 (11). In addition, marrow mesenchymal cell support of osteoclastogenesis is increased because of the increased production of macrophage colony-stimulating factor (M-CSF) and receptor activator of nuclear factor- κ B ligand (RANKL) (12). Thus, normal aging changes the status of marrow MSC with respect to both their differentiation potential and their production of specific signaling molecules. Such molecular changes contribute to the formation of the specific microenvironment necessary for the maintenance of bone homeostasis.

Multiple alternate PPAR γ transcripts translate to two protein isoforms, PPAR γ 1 and PPAR γ 2. PPAR γ 1 is expressed in many cell types, including osteoblasts, whereas PPAR γ 2 is specifically expressed in adipocytes and is responsible for the regulation of both differentiation and function (10, 13).

First Published Online March 1, 2007

Abbreviations: BMC, Bone mineral content; BMD, bone mineral density; CFU-OB, colony-forming units for osteoblast; 1,25(OH) $_2$ D $_3$, 1,25-dihydroxyvitamin D $_3$; microCT, microcomputed tomography; MSC, mesenchymal stem cell; PPAR γ , peroxisome proliferator-activated receptor- γ ; RANKL, receptor activator of nuclear factor- κ B ligand; Runx2, runt-related transcription factor 2; TRAP, tartrate-resistant acid phosphatase; TZD, thiazolidinedione.

Endocrinology is published monthly by The Endocrine Society (<http://www.endo-society.org>), the foremost professional society serving the endocrine community.

PPAR γ activation requires heterodimerization with another nuclear receptor, retinoid X receptor (RXR), and binding of a specific ligand (14). Ligands for PPAR γ include polyunsaturated fatty acids, oxidized metabolites of prostaglandin J₂, certain phospholipids, and antidiabetic drugs such as thiazolidinediones (TZD) (14). Currently, two TZD, rosiglitazone and pioglitazone, are used to control glucose levels in diabetic patients.

An essential role for PPAR γ in the maintenance of bone homeostasis has been demonstrated in several animal models of either bone accrual or bone loss, depending on the status of PPAR γ activity (2, 3, 15–18). In models of bone accrual, a decrease in PPAR γ activity in either heterozygous PPAR γ -deficient mice or mice carrying a hypomorphic mutation in the PPAR γ gene locus led to increased bone mass due to increased osteoblast number (3, 17). Moreover, the rate of bone loss with aging was significantly lower in heterozygous PPAR γ -deficient mice compared with the control animals, which possessed both chromosomal copies of PPAR γ (3). In contrast, in models of bone loss due to PPAR γ activation, administration of rosiglitazone to mice and rats resulted in significant decreases in bone mineral density (BMD) and bone volume and changes in bone microarchitecture (2, 15, 16, 18). This treatment-induced bone loss was associated with changes in the structure and function of bone marrow, such as a decreased number of osteoblasts and an increased number of adipocytes (2, 18).

In humans, 4-yr follow-up data from the Health, Aging, and Body Composition observational study revealed that TZD administration results in progressive bone loss in diabetic older postmenopausal women but not in older diabetic men (19). In addition, the clinical evaluation of PPAR γ gene polymorphisms strongly suggests a role in the regulation of bone mass in humans (20). A silent C→T transition in exon 6 results in a lower bone density and a predisposition to osteoporosis (20). Several novel polymorphisms were also identified in the coding region of PPAR γ that, particularly in women, correlated with BMD independently of body weight and type 2 diabetes in the Framingham Offspring Study (21).

Because PPAR γ expression increases in marrow MSC with aging, the effect of PPAR γ activation by rosiglitazone on the skeletons of growing, adult, and aging animals was examined. Rosiglitazone treatment resulted in distinctive changes in bone microarchitecture and strength, as well as age-dependent changes in the function of the mesenchymal compartment of bone marrow. These changes included decreased osteoblast number in adult, increased osteoclast number in aged, and an increased number of marrow adipocytes in all ages of animals analyzed. Moreover, rosiglitazone suppressed the multipotential phenotype of adult marrow MSC to a level comparable to that observed in aged animal marrow. The bone loss that occurs due to rosiglitazone treatment shares the features of, and involves mechanisms similar to, age-related bone loss.

Materials and Methods

Experimental animals and treatment regime

Nondiabetic male C57BL/6 mice were obtained from the colony maintained by the National Institute on Aging under contractual agreement with Harlan Sprague Dawley, Inc. (Indianapolis, IN). Animals,

identified by punched ears, were housed (four per cage) with free access to water and were maintained at a constant temperature, on a 12-h light, 12-h dark cycle. The animal treatment and care protocols conformed to National Institutes of Health Guidelines and were performed using a University of Arkansas for Medical Sciences Institutional Animal Care and Use Committee-approved protocol.

Animals were grouped and referred to as follows: young (1 month old), 10 animals per group, and adult (6 months old) and old (24 months old), eight animals per group. Animals were fed 5 g of food per day per animal with pelleted chow (F05072; Bio-Serv, Frenchtown, NJ) supplemented with rosiglitazone maleate (Avandia; GlaxoSmithKline, King of Prussia, PA) at the concentration of 0.14 mg/g chow. The control group was fed the same amount of nonsupplemented chow. Animals were fed every other day for 7 wk, and food and rosiglitazone intake per cage and body weights of individual animals were monitored. To permit dynamic bone histomorphometric measurements, mice were injected ip with 30 μ g/g body weight of tetracycline 7 and 2 d before being killed as described (2).

Measurements of serum metabolic parameters

Blood was collected by cardiac puncture at the time of killing and allowed to clot, and serum was collected by centrifugation. Plasma glucose levels were measured using Accu-Check Advantage Blood Glucose Meter (Roche Diagnostic Corp., Indianapolis, IN). Serum insulin levels were determined using the Mouse Insulin ELISA kit (ALPCO, Windham, NH), serum bone-specific alkaline phosphatase levels were determined in *p*-nitrophenol reaction using Phosphatase Substrate (Sigma Chemical Co., St. Louis, MO) in the presence of 10 mM L-phenylalanine to inhibit any circulating intestinal alkaline phosphatase, and serum C-telopeptide degradation products from type I collagen were measured using RatLaps ELISA kit (Nordic Bioscience Diagnostics, Herlev, Denmark).

BMD measurements

BMD was determined using the Piximus instrument and software version 1.46 (GE Lunar, Madison, WI). Mice were anesthetized and scanned at the beginning of the experiment and before the onset of rosiglitazone treatment, an intermediate time point (4 wk), and at killing (7 wk). Total body BMD (g/cm²), excluding the head region, was obtained from each scan, and the percent change in BMD was determined as described (2). Internal variations of repeated measures of total murine body BMD have been determined to be 1.7–2.0%.

Microcomputed tomography (microCT) analysis

After killing, the right tibia of each animal was dissected and fixed in Millonig's phosphate-buffered 10% formalin (pH 7.4). After 24 h, the tibia was dehydrated successively in 70, 95, and 100% ethanol and measured without additional sample preparation in a microCT 40 (Scanco Medical, Bassersdorf, Switzerland), as described (2, 22).

Mechanical testing

The fifth lumbar vertebrae (L5) was harvested and used for biomechanical testing. The compressive strength of L5 vertebrae were determined in a single load-to-failure compression test as we have previously described (23) using a MTS 858 Bionex Test Systems load frame (MTS, Eden Prairie, MN) with computer control, data logging, and calculations of load-to-failure using TestWorks version 4.0 (MTS). The load frame was operated at a constant rate of 0.1 mm/sec with load and displacement recorded at 100 Hz. Load-to-failure was recorded as the load after a 2% drop from peak load.

Bone histomorphometry

After microCT data collection, the same tibiae were embedded undecalcified in methyl methacrylate and sectioned at 4 μ m using a tungsten carbide steel knife on an automatic, retractable Microtom 355 with a D-profile. Adjacent sections were stained with Masson trichrome, Goldner trichrome, von Kossa, and two were left unstained for evaluation of tetracycline labeling evaluation (2, 24). Osteoclasts were quan-

tified in sections stained for tartrate-resistant acid phosphatase (TRAP), with osteoclasts identified as TRAP⁺ multinucleated cells, adjacent to bone. All histomorphometric examination was performed in a blinded, nonbiased manner using a computerized semiautomated OsteoMeasure system (OsteoMetrics Inc., Atlanta, GA) as previously described (2). Briefly, all measurements were confined to the secondary spongiosa and restricted to an area between 700 and 1500 μm distal to the growth plate-metaphyseal junction of the proximal tibia. A minimum of 25 fields in the proximal tibia were evaluated (2). Static measurements and dynamic lengths of single- and double-labeled bone surfaces were obtained (2, 24) and reported using the terminology recommended by the Histomorphometry Nomenclature Committee of ASBMR (25). Adipocyte number in the metaphysis of the proximal tibia was measured on five different microscopic fields at $\times 20$ magnification.

RNA isolation and quantitative real-time RT-PCR analysis

Total RNA was isolated from the left tibia of each animal, and gene expression in the entire bone was analyzed using quantitative real-time RT-PCR. Immediately after the animal was killed, the tibia was cleaned of all remaining soft tissue, cut into pieces, and homogenized in the presence of TRIzol Reagent (Life Technologies, Grand Island, NY) followed by RNA isolation as described by the manufacturer. Real-time PCR were performed as described (22).

Gene expression was analyzed using the following primer pairs: RANKL (forward, ATGCTGCCAGCATCCCA; reverse, CCCAGCCTC-GATCGTGG), OPG (forward, TCCGGCGTGGTGCAAG; reverse, AGAACCCATCTGGACATTTTTT), PPAR γ (forward, TCATCTCA-GAGGGCCAAGGA; reverse, CACCAAAGGGCTTCCGC), PPAR γ 2 (forward, AAAGTCTGGGAGATTCTCTGTG; reverse, GAAGTGT-CATAGGCAGTGCA), and 18S rRNA (forward, TTCGAACGCTGC-CCTATCAA; reverse, ATGGTAGGCACGGCGACTA).

Murine primary bone marrow cultures and the assessment of osteoblast and adipocyte differentiation

Bone marrow cultures were established from femur marrow aspirates as described (22). Bone marrow was isolated from individual mice ($n = 8$) and seeded separately in triplicate at a density of 2.5×10^5 cells/ cm^2 on six-well tissue culture plates (Becton Dickinson Labware, Franklin Lakes, NJ) in α -MEM (Life Technologies) supplemented with 15% fetal bovine serum (Hyclone, Logan, UT). To measure the number of osteoblastic progenitors (CFU-OB), cells were maintained in osteoblastic medium (basal medium supplemented with 0.2 mM ascorbic acid and 10 mM β -glycerophosphate; Sigma) for 28 d with one half of the medium changed every 6 d. Mineralization was determined by von Kossa staining as described (24). To measure the number of adipocytic progenitors, after the initial 10 d of growth, cultures were exposed for the next 3 d to the medium supplemented with 10^{-6} M rosiglitazone (Tularik Inc., South San Francisco, CA). Fat-containing cells were visualized with Oil Red O staining, and adipogenesis was quantified by enumerating colonies containing at least 10% Oil Red O-positive cells (26).

The assessment of the multipotential phenotype of MSC was performed as described (10). Briefly, murine bone marrow adherent cells were grown in the presence of basal medium for 10 d followed by an additional 3 d of growth either in the same medium or in basal medium supplemented with 10^{-6} M rosiglitazone. Next, all medium was changed to pro-osteoblastic medium (basal medium supplemented with 0.2 mM ascorbic acid and 10 mM β -glycerophosphate). All cultures were then allowed to grow for an additional 28 d. The number of mineralized CFU-OB was enumerated after von Kossa staining.

Osteoclastogenesis

To assess the effects of rosiglitazone treatment on mesenchymal cell support for osteoclastogenesis, coculture of murine bone marrow and immortalized murine marrow mesenchymal cells stably transfected with PPAR γ 2 expression construct (U-33/ γ 2 cells) (10) were used. The U-33/ γ 2 cells are rosiglitazone-responsive, endogenously express RANKL and OPG, and support recruitment and development of TRAP-positive osteoclasts from the fraction of nonadherent primary bone marrow cells. U-33/ γ 2 cells were seeded (1×10^4 cells per well) on

48-well tissue culture plates (Becton Dickinson Labware, Franklin Lakes, NJ) in α -MEM supplemented with 10% fetal bovine serum.

In the first set of experiments, after 24 h of growth, cells were pretreated with either vehicle (dimethylsulfoxide) or 10^{-6} M rosiglitazone for 2 d followed by the addition of the nonadherent fraction of primary murine bone marrow cells (2.5×10^5 cells per well) as a source of osteoclast progenitors. Nonadherent cells were collected from primary murine bone marrow cultures, established 2 d earlier, by plating marrow isolates at 2×10^5 cells/ cm^2 . The cocultures of nonadherent murine bone marrow cells and U-33/ γ 2 cells, pretreated or not with rosiglitazone (10^{-6} M), were grown in the presence of either nonsupplemented α -MEM or medium supplemented with 10^{-8} M 1,25-dihydroxyvitamin D₃ [(1,25(OH)₂D₃] (Sigma) in quadruplicate. In the second series of experiments, cocultures of U-33/ γ 2 cells and nonadherent bone marrow cells were either supplemented or not with 10^{-6} M rosiglitazone (as above) in the presence or absence of 10^{-8} M 1,25(OH)₂D₃ for the remainder of the experiment. Cultures were grown for 6 d with a half medium change on d 3 followed by staining for TRAP according to the manufacturer (Acid Phosphatase Leukocyte Kit; Sigma). TRAP-positive (TRAP⁺) multinucleated cells per well were enumerated. In addition, the number of nuclei per TRAP⁺ multinucleated cell was measured.

Statistical analysis

Statistically significant differences between groups were detected using one-way ANOVA followed by *post hoc* analysis by Student-Neuman-Keuls within the SigmaStat software (SPSS, Inc., Chicago, IL) after establishing homogeneity of variance and the normal distribution of the data. Data that were not normally distributed were analyzed by Mann-Whitney *U* test on the ranks and Dunn's *post hoc* tests using SigmaStat software. In all cases, $P < 0.05$ was considered significant. Histomorphometric data were analyzed using SigmaStat or SAS software (SAS Institute Inc., Cary, NC) (2). All values are presented as the mean \pm sd. Differences between group means in all histomorphometric studies were evaluated with Student's *t* test or ANOVA after *P* values were adjusted with Bonferroni's correction (2).

Results

The C57BL/6 mouse strain is a commonly accepted model of bone aging (27). Changes that occur in the tibial metaphysis and diaphysis in male C57BL/6 mice closely resemble changes that occur in human bone with aging (27, 28). Bone growth in C57BL/6 males, measured as increasing BMD, occurs during the first 3–4 months of life, peaks at around 5–6 months, and is followed by a gradual decline that continues throughout the lifespan of the animal (~26–36

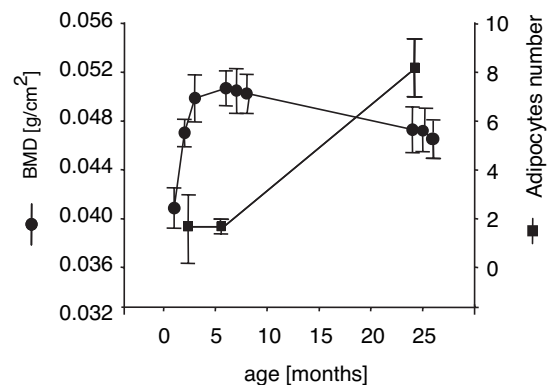


FIG. 1. The inverse relationship between BMD and marrow adipocytes. BMD (●) and the total number of marrow adipocytes in tibia (■) were measured as a function of aging in C57BL/6 mice. Adipocyte number was measured in the metaphysis of the proximal tibia. Numbers represent a mean of five fields at magnification $\times 20$. Data were collected from 10 young, eight adult, and eight old animals.

months) (Fig. 1). Similar to humans, bone loss in older animals is accompanied by a corresponding increase in the number of marrow adipocytes (Fig. 1). There is no significant difference in adipocyte number in young growing animals and adult animals at peak BMD; however, adipocyte numbers increase sharply in old animals and are positively correlated with the decreased BMD observed (Fig. 1).

Age-related effects of rosiglitazone on bone mass

Because osteoblasts and adipocytes share a common mesenchymal progenitor and expression of the adipocyte-related PPAR γ 2 isoform increases in undifferentiated MSC with aging (11), we hypothesized that PPAR γ activation after rosiglitazone treatment will induce bone loss as a function of age. Therefore, the skeletal responses to rosiglitazone of young (1 month), adult (6 months), and old (24 months) animals were examined. Animals in each age group were fed a diet supplemented with rosiglitazone for 7 wk. At the end of 7 wk, animals were 3, 8, and 26 months old, respectively. The average daily dose of rosiglitazone, calculated at the end of the experiment, was not significantly different between groups (young, 17.4 μ g/g body weight; adult, 18.7 μ g/g; and old, 16.1 μ g/g). However, the differences between the cumulative doses in each group (daily dose \times duration of experiment) were significant ($P < 0.05$) (young, 974.4 μ g/g body weight; adult, 916.3 μ g/g; and old, 788.9 μ g/g). Thus, young animals received the largest cumulative dose of rosiglitazone, whereas old animals received the smallest.

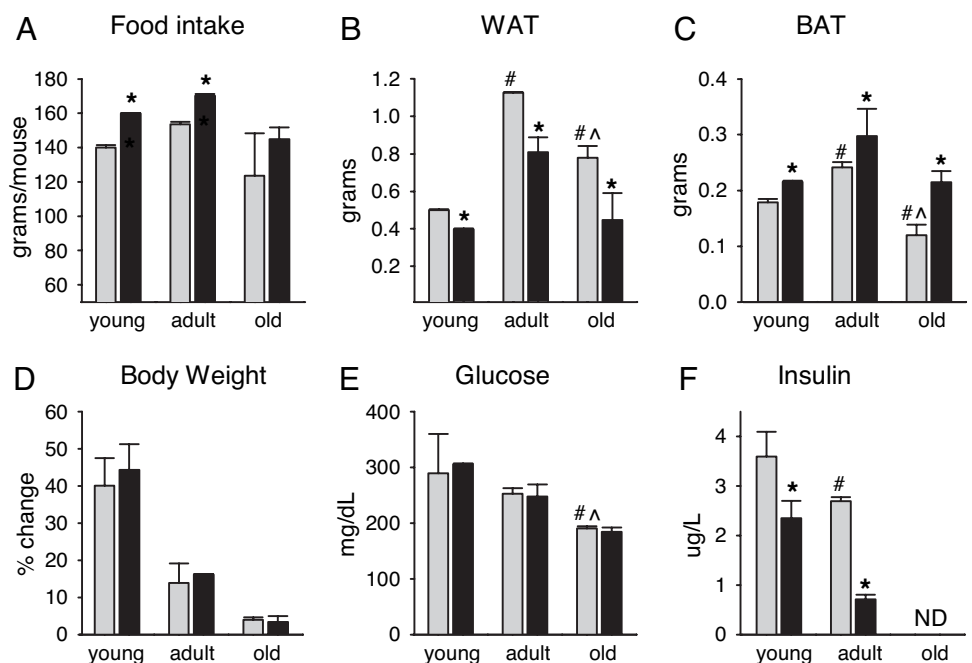
Animals that received a diet supplemented with rosiglitazone responded with higher food intake, decreased weight of epididymal or white fat, and increased weight of interscapular or brown fat (Fig. 2, A–C). However, in contrast to type 2 diabetic patients and animal models, rosiglitazone treatment of nondiabetic animals did not change body weight or alter serum glucose levels (Fig. 2, D and E) (29). Interestingly, insulin levels were significantly compromised,

suggesting activation of compensatory mechanisms in nondiabetic animals, which stabilized blood glucose levels in the presence of rosiglitazone (Fig. 2F). No changes in serum levels for bone-specific alkaline phosphatase or C-telopeptide were detected (data not shown).

A change in global BMD, calculated as a percent fraction between an individual animal's BMD value at the beginning and at the end of the experiment, indicated that rosiglitazone decreased BMD in adult and old, but not young, animals (Fig. 3A). However, measurement of the changes in bone mineral content (BMC) demonstrated a negative effect of rosiglitazone in all age groups tested (Fig. 3B). Furthermore, detailed examination of the kinetics of bone loss accompanying rosiglitazone treatment demonstrated that the majority of the bone loss in adult animals (\sim 63% of total bone loss) occurred during the final 3 wk of rosiglitazone treatment, whereas the bone loss in old animals (\sim 70% of total bone loss) occurred during the initial 4 wk of treatment (Fig. 3, C and D, respectively). Such a time-dependent difference in the response to rosiglitazone treatment suggests that different cellular targets and/or different mechanisms are responsible for the rosiglitazone-induced bone loss in adult and old animals.

Next, the effect of rosiglitazone treatment on vertebral bone strength was determined. Rosiglitazone treatment significantly decreased load-to-failure of L5 vertebral bodies in adult, but not young, animals to a similar level to that of aged control animals (Fig. 3E). The decrease in mechanical strength was positively correlated with the decrease in BMD in rosiglitazone-treated adult animals. As expected, bone strength in aged control animals was significantly compromised compared with both young and adult animals. Rosiglitazone administration further decreased vertebral strength in aged animals; however, the values did not achieve statistical significance (Fig. 3E).

FIG. 2. Changes in metabolic parameters as function of aging and rosiglitazone administration. A, Total food intake per mouse during the experiment; B and C, average weight of white epididymal fat (WAT) (B) and brown interscapular fat (BAT) (C) measured at the end of the experiment; D, average change in body weight calculated as a percent change between the beginning and the end of the experiment; E, level of blood glucose measured at the end of the experiment; F, serum insulin levels measured at the end of the experiment. Data were collected from the following number of animals in each group: young, 10 control and 10 rosiglitazone; adult, eight control and eight rosiglitazone; old, eight control and seven rosiglitazone. Gray bars, control; black bars, rosiglitazone. ND, No data; *, $P < 0.05$ vs. control; #, $P < 0.05$ vs. young; \wedge , $P < 0.05$ vs. adult.



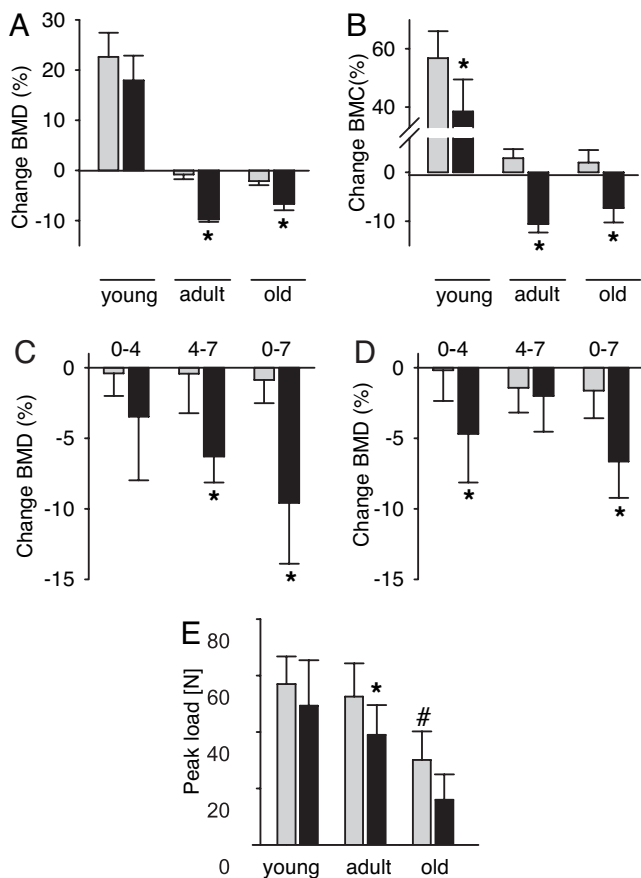


FIG. 3. Changes in BMD, BMC, and bone strength as a function of rosiglitazone treatment and aging. Changes in BMD and BMC are expressed as a percent change at the end of the experiment compared with the values at the beginning of the experiment. A, Change in global BMD; B, change in global BMC; C and D, kinetics of the change in global BMD of adult (C) and old (D) animals. Values represent changes that occurred during the first 4 wk of treatment (0–4), between the fourth and seventh week of treatment (4–7), and between the beginning and the end of treatment (0–7). E, Vertebral bone strength was measured at the end of the experiment as described in *Materials and Methods*. Data were collected from the following number of animals in each group: young, 10 control and 10 rosiglitazone; adult, eight control and eight rosiglitazone; old, eight control and seven rosiglitazone. Gray bars, control; black bars, rosiglitazone. *, $P < 0.05$ vs. control; #, $P < 0.05$ vs. young.

Analysis of bone microarchitecture by microCT

Analysis of trabecular bone microarchitecture in the proximal tibia using microCT revealed that rosiglitazone induced changes in bone architecture that paralleled the changes observed with aging (Fig. 4). In adult animals, both aging and rosiglitazone treatment decreased bone volume fraction (Fig. 4B) and trabecular number (Fig. 4C) and increased trabecular spacing (Fig. 4D). No changes in connectivity density (Fig. 4E) or trabecular thickness were seen with rosiglitazone treatment in young animals; however, rosiglitazone treatment significantly decreased trabecular thickness in adult animals (Fig. 4F). No changes in trabecular bone microarchitecture were observed in young animals treated with rosiglitazone. In old animals treated with rosiglitazone, bone loss was so extensive that little or no trabecular bone remained, making analysis by microCT problematic and unreliable statistically.

Histomorphometric analysis of bone formation and bone resorption parameters

Histomorphometric analysis (Table 1) demonstrated the cellular basis for the age-dependent effect of rosiglitazone to increase bone loss. In young growing animals, rosiglitazone treatment significantly decreased bone formation rate. No other osteoblast parameters in young mice were significantly affected. Rosiglitazone did not affect osteoclast number in either young or adult animals (Table 1). However, in adult animals, rosiglitazone decreased the number of osteoblasts resulting in a decreased mineral apposition rate and ultimately decreased bone formation rate (Table 1), as we and others have shown previously (2, 18).

In contrast, the cellular basis for bone loss in rosiglitazone-treated aged animals was distinctly different. As expected, parameters of bone formation, such as bone formation rate, mineral apposition rate, and osteoblast number, were greatly compromised in old nontreated animals. Rosiglitazone administration had no significant effect on any measured osteoblast parameter in old animals. However, in contrast to adult animals, in old rosiglitazone-treated animals, bone loss was directly related to the significant increase in osteoclast number (Table 1). These results suggest that rosiglitazone treatment affects distinct cellular bone compartments in adult and aged animals.

To assess the effect of aging and rosiglitazone on the support for osteoclastogenesis, the ratio of RANKL to OPG mRNA expression was examined (30–32) (Fig. 5A). Because RANKL and OPG are expressed in the marrow by cells of different lineages and support osteoclastogenesis in a paracrine fashion, the expression of their transcripts was measured in the intact bone of experimental animals as opposed to the specific marrow cellular compartment. As shown in Fig. 5, B and C, during aging, relative levels of RANKL mRNA increase, whereas levels OPG mRNA decrease, respectively. This results in the increased RANKL-to-OPG ratio in the tibia of both adult and old animals but not in the tibia of young animals (Fig. 5A). This ratio was further increased in the bone of rosiglitazone-treated animals (Fig. 5A). The observed increase in the RANKL-to-OPG ratio in rosiglitazone-treated animals was entirely due to increased RANKL mRNA expression, because no significant change in OPG mRNA expression was detected (Fig. 5, B and C, respectively). Interestingly, the RANKL-to-OPG ratio was also increased in the bone of adult rosiglitazone-treated animals in the absence of increased bone resorption (Fig. 5A; see Table 1). However, the relative expression of RANKL in adult animals was lower, and OPG expression higher, compared with the expression levels in the bone of old rosiglitazone-treated animals (Fig. 5, B and C, respectively). These data may explain the observed lack of increase in osteoclastogenesis in rosiglitazone-treated adult animals *in vivo*. Rosiglitazone did not affect RANKL-to-OPG ratio or RANKL or OPG expression in young animals, which is consistent with the lack of effect of this drug on bone resorption in young animals.

Rosiglitazone increases mesenchymal cell support for osteoclastogenesis *in vitro*

The effect of rosiglitazone on the support of osteoclastogenesis by marrow MSC was examined using U-33/ γ 2 cells, a mesenchymal cell line, in which osteoblast and adipocyte

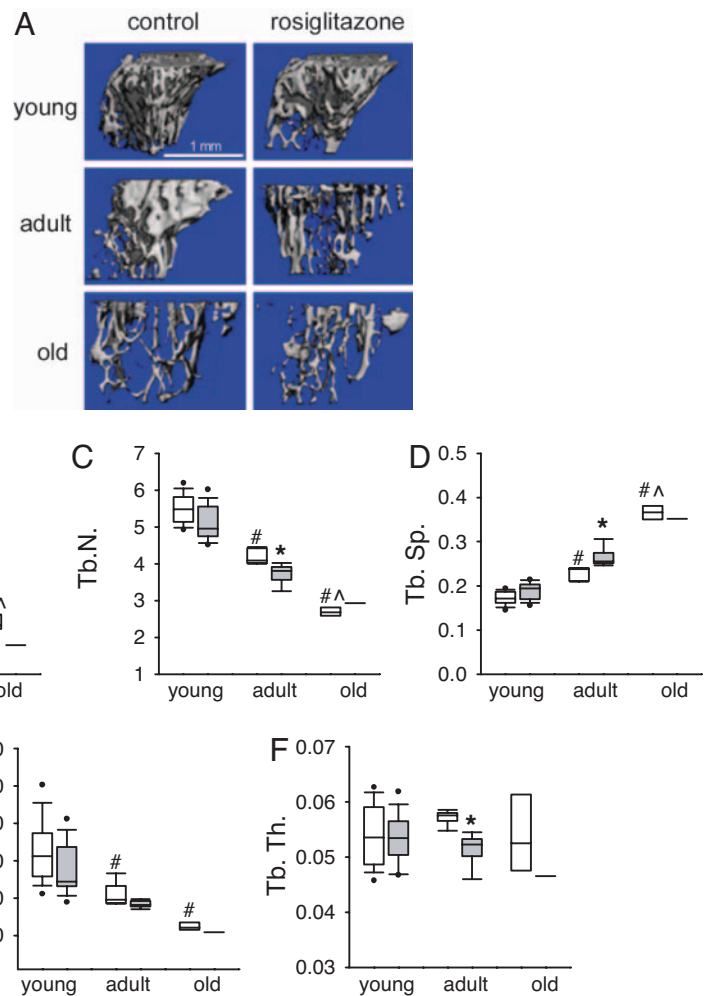


FIG. 4. MicroCT analysis of bone microarchitecture. **A**, Three-dimensional reconstructions of microCT data from the tibiae of control and rosiglitazone-treated young, adult, and old animals (scale bar, 1 mm); **B**, bone volume per tissue volume (BV/TV); **C**, trabecular number (Tb.N.); **D**, trabecular spacing (Tb.SP.); **E**, connectivity density (Conn.D.); **F**, trabecular thickness (Tb.Th.). The following number of tibiae were analyzed in each group: young, 10 control and 10 rosiglitazone; adult, five control and five rosiglitazone; old, four control and one rosiglitazone. In old animals treated with rosiglitazone, bone loss was so extensive that little or no trabecular bone remained, making analysis by microCT reliable for only one experimental tibia. The data are presented as box plots with plotted median (horizontal lines) and 5th/95th percentile of outliers (dots). White boxes, control; gray boxes, rosiglitazone. *, $P < 0.05$ vs. control; #, $P < 0.05$ vs. young animals; ^, $P < 0.05$ vs. adult animals.

differentiation are under the control of PPAR γ 2 (10, 26). U-33/ γ 2 cells support the recruitment and differentiation of osteoclast-like cells in coculture with nonadherent bone marrow cells, as measured by TRAP⁺ multinucleated cell formation (Table 2), due to the endogenous expression of RANKL. Rosiglitazone treatment (10^{-6} M) completely inhib-

ited U-33/ γ 2 support of osteoclast development, whereas treatment of U-33/ γ 2 cells with $1,25(\text{OH})_2\text{D}_3$ (10^{-8} M) significantly enhanced osteoclastogenesis (Table 2). Interestingly, pretreatment of U-33/ γ 2 cells with rosiglitazone (10^{-6} M) followed by treatment with $1,25(\text{OH})_2\text{D}_3$ (10^{-8} M) significantly increased total osteoclast-like cell number compared

TABLE 1. Effect of rosiglitazone and aging on cancellous bone in the proximal tibia

Parameter	Young		Adult		Old	
	Control	Rosiglitazone	Control	Rosiglitazone	Control	Rosiglitazone
Bone area/tissue area (%)	7.0 \pm 2.5	4.9 \pm 1.4	8.2 \pm 3.4	4.9 \pm 2.2	2.5 \pm 4.4 ^{b,c}	1.3 \pm 1.8
Trabecular width (μm)	36.6 \pm 2.1	36.7 \pm 3.2	37.1 \pm 3.2	36.6 \pm 6.1	29.3 \pm 4.3	31.1 \pm 5.8
Trabecular spacing (μm)	325 \pm 121	366 \pm 102	425 \pm 183	693 \pm 145 ^a	477 \pm 89 ^b	779 \pm 176 ^a
Trabecular number (n/mm ² tissue area)	1.3 \pm 0.7	1.6 \pm 0.5	1.8 \pm 0.3	1.5 \pm 0.7	0.8 \pm 0.3 ^c	1.1 \pm 0.7
Osteoid width (μm)	2.1 \pm 0.3	2.3 \pm 0.3	2.4 \pm 0.3	2.1 \pm 0.3	1.7 \pm 0.3	1.9 \pm 0.3
Osteoblast number (n/mm ² tissue area)	76.2 \pm 12.1	34.6 \pm 22.7	83.2 \pm 21.1	46.6 \pm 12.7 ^a	21 \pm 12.7 ^{b,c}	24 \pm 11.2
Osteoblast number (n/mm bone perimeter)	23.3 \pm 6.2	19.2 \pm 12.2	21.3 \pm 7.2	11.2 \pm 4.1	3.2 \pm 1.1 ^{b,c}	3.6 \pm 1.7
Mineral apposition rate ($\mu\text{m}/\text{d}$)	1.11 \pm 0.2	0.8 \pm 0.2	2.82 \pm 0.3 ^b	0.9 \pm 0.4 ^a	1.0 \pm 0.3 ^c	0.9 \pm 0.4
Bone formation rate/bone perimeter ($\mu\text{m}^2/\mu\text{m}\cdot\text{d}$)	0.135 \pm 0.042	0.069 \pm 0.029 ^a	0.204 \pm 0.101	0.077 \pm 0.039 ^a	0.08 \pm 0.04 ^c	0.07 \pm 0.02
Osteoclast number (n/mm ² tissue area)	5.1 \pm 0.8	5.2 \pm 1.2	6.2 \pm 0.7	5.9 \pm 1.1	6.9 \pm 0.7 ^b	9.5 \pm 1.2 ^a
Osteoclast number (n/mm bone perimeter)	2.0 \pm 0.2	1.7 \pm 0.5	3.1 \pm 0.4 ^b	3.4 \pm 0.7	2.9 \pm 0.1	4.1 \pm 0.7 ^a

The following number of animals in each group was analyzed: young, five control and five rosiglitazone; adult, five control and five rosiglitazone; old, five control and three rosiglitazone.

^a $P < 0.05$ vs. age-matched control.

^b $P < 0.05$ vs. control young.

^c $P < 0.05$ vs. control adult.

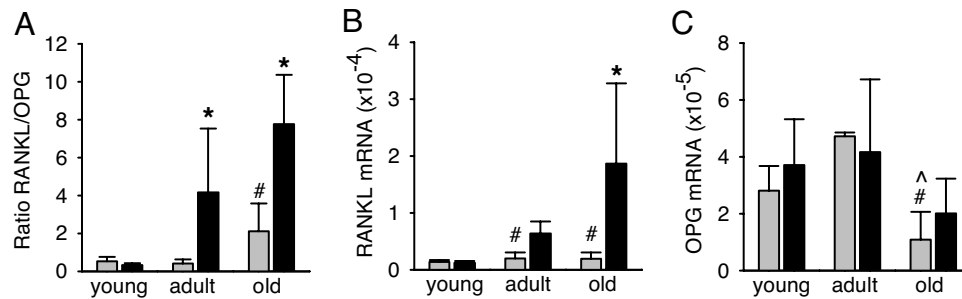


FIG. 5. Measurement of the RANKL and OPG mRNA expression in bone as a function of age and rosiglitazone administration. Total RNA was extracted from the proximal tibia and analyzed by real-time PCR. A, Determination of the RANKL/OPG mRNA ratio; B, RANKL mRNA expression levels; C, OPG mRNA expression levels. Tibiae RNA were extracted from the following number of animals in each group: young, four control and four rosiglitazone; adult, three control and four rosiglitazone; old, four control and four rosiglitazone. Gray bars, control; black bars, rosiglitazone. *, $P < 0.05$ vs. control; #, $P < 0.05$ vs. young animals; λ , $P < 0.05$ vs. adult animals.

with treatment with $1,25(\text{OH})_2\text{D}_3$ alone (Table 2; experiment type 1). Furthermore, analysis of cellular morphology demonstrated that under basal conditions, U-33/ γ 2 cells modestly supported the recruitment of TRAP⁺ cells (one to three nuclei per cell), whereas in the presence of $1,25(\text{OH})_2\text{D}_3$, the number of more mature multinucleated TRAP⁺ cells (33) (four to 19 or ≥ 20 nuclei per cell) was significantly increased (Table 2). Pretreatment with rosiglitazone followed by treatment with $1,25(\text{OH})_2\text{D}_3$ increased not only the total number of TRAP⁺ osteoclast-like cells but also the number of osteoclast-like cells containing four or more nuclei (Table 2).

To further examine the functional consequences of rosiglitazone and $1,25(\text{OH})_2\text{D}_3$ on osteoclast-like cell formation, U-33/ γ 2 and nonadherent bone marrow cells were cocultured in the presence of both $1,25(\text{OH})_2\text{D}_3$ and rosiglitazone (Table 2; experiment type 2). As shown in Table 2, the simultaneous combination of rosiglitazone and $1,25(\text{OH})_2\text{D}_3$ decreased the total number of TRAP⁺ osteoclast-like cells compared with treatment with $1,25(\text{OH})_2\text{D}_3$ alone. This result is entirely consistent with the inhibitory effects of rosiglitazone on osteoclast precursors observed by others (34–36).

The change in U-33/ γ 2 cell support of osteoclastogenesis after pretreatment with rosiglitazone positively correlated with the observed changes in the RANKL-to-OPG ratio (Fig. 6A). Treatment of U-33/ γ 2 cells with rosiglitazone alone decreased the RANKL-to-OPG ratio. In contrast, the RANKL-to-OPG ratio was significantly increased by $1,25(\text{OH})_2\text{D}_3$ treatment and was further enhanced in cells

pretreated with rosiglitazone before the addition of $1,25(\text{OH})_2\text{D}_3$ (Fig. 6A). Rosiglitazone increased the RANKL-to-OPG ratio primarily by an up-regulation of RANKL mRNA (Fig. 6, B and C). A similar effect of rosiglitazone on RANKL and OPG mRNA expression was observed in U-33/ γ 2 cells simultaneously treated with both rosiglitazone and $1,25(\text{OH})_2\text{D}_3$ (data not shown). Collectively, these results suggest that PPAR γ may have a dual role in the regulation of osteoclastogenesis. PPAR γ activation increases the support for osteoclastogenesis mediated by $1,25(\text{OH})_2\text{D}_3$ -stimulated increases in RANKL expression in mesenchymal cells and also affects the recruitment of osteoclast-committed precursors from the pool of hematopoietic cells.

Rosiglitazone induces changes in bone histology characteristic of aging bone

Histological examination of the proximal tibia of young, adult, and aged animals revealed that rosiglitazone-induced changes in the bone and marrow compartments closely resemble age-induced changes (Fig. 7A). With aging, bone volume in the primary spongiosa and metaphysis decreases and the growth plate closes (28). Marrow infiltration into the epiphysis becomes more pronounced, leading to the fusion of both the metaphyseal and epiphyseal areas and replacement of the bone space with marrow infiltrated with fat cells (Fig. 7A) (28). A similar pattern of histological changes is seen in animals treated with rosiglitazone. The histological appearance of the proximal tibia of adult animals after 7 wk of rosiglitazone treatment

TABLE 2. The effect of $1,25(\text{OH})_2\text{D}_3$ and rosiglitazone on osteoclast development in co-culture of non-adherent bone marrow cells and U-33/ γ 2 cells

Treatment	Experiment type 1 ^a				Experiment type 2 ^b			
	1–3 ^c	4–19 ^c	>20 ^c	Total ^d	1–3 ^c	4–19 ^c	>20 ^c	Total ^d
Vehicle	25.7 ± 2.1 ^e	0	0	25.7 ± 2.1 ^e	32.0 ± 6.0 ^e	0	0	32.0 ± 6.0 ^e
Rosiglitazone	0	0	0	0	0	0	0	0
$1,25(\text{OH})_2\text{D}_3$	288.8 ± 25.5	162.8 ± 27.3	3.0 ± 1.4	454.5 ± 18.9	325.0 ± 13.7	240.3 ± 33.8	4.8 ± 1.7	570.0 ± 42.3
Rosiglitazone + $1,25(\text{OH})_2\text{D}_3$	166.3 ± 17.4 ^e	313.5 ± 24.8 ^e	73.8 ± 6.2 ^e	553.5 ± 30.5 ^e	102.5 ± 7.9 ^e	151.0 ± 7.5 ^e	24.8 ± 6.4 ^e	278.3 ± 14.4 ^e

^a U-33/ γ 2 cells were pretreated with 10^{-6} M rosiglitazone for 2 d followed by a medium change and addition of 10^{-8} M $1,25(\text{OH})_2\text{D}_3$ and nonadherent bone marrow cells followed by TRAP staining after 6 d of growth.

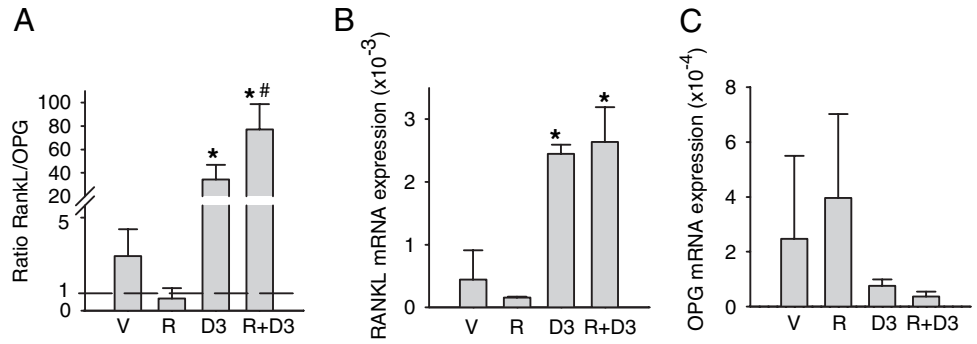
^b Osteoclastogenesis in the presence of 10^{-6} M rosiglitazone and 10^{-8} M $1,25(\text{OH})_2\text{D}_3$ followed by TRAP staining after 6 d of growth.

^c Number of nuclei per TRAP⁺ cell.

^d Total number of TRAP⁺ cells per well.

^e $P < 0.05$ vs. $1,25(\text{OH})_2\text{D}_3$.

FIG. 6. Rosiglitazone and 1,25(OH)₂D₃ effects on RANKL and OPG expression in U-33/γ2 cells. U-33/γ2 cells were cultured in the presence of vehicle (V), or 10⁻⁶ M rosiglitazone (R), 10⁻⁸ M 1,25(OH)₂D₃ (D3), or both (R+D3) for 7 d followed by total RNA isolation. The levels of RANKL and OPG gene expression were measured using real-time PCR. A, RANKL/OPG expression ratio; B, RANKL mRNA expression; C, OPG mRNA expression. *, *P* < 0.05 vs. vehicle; #, *P* < 0.05 vs. 1,25(OH)₂D₃.

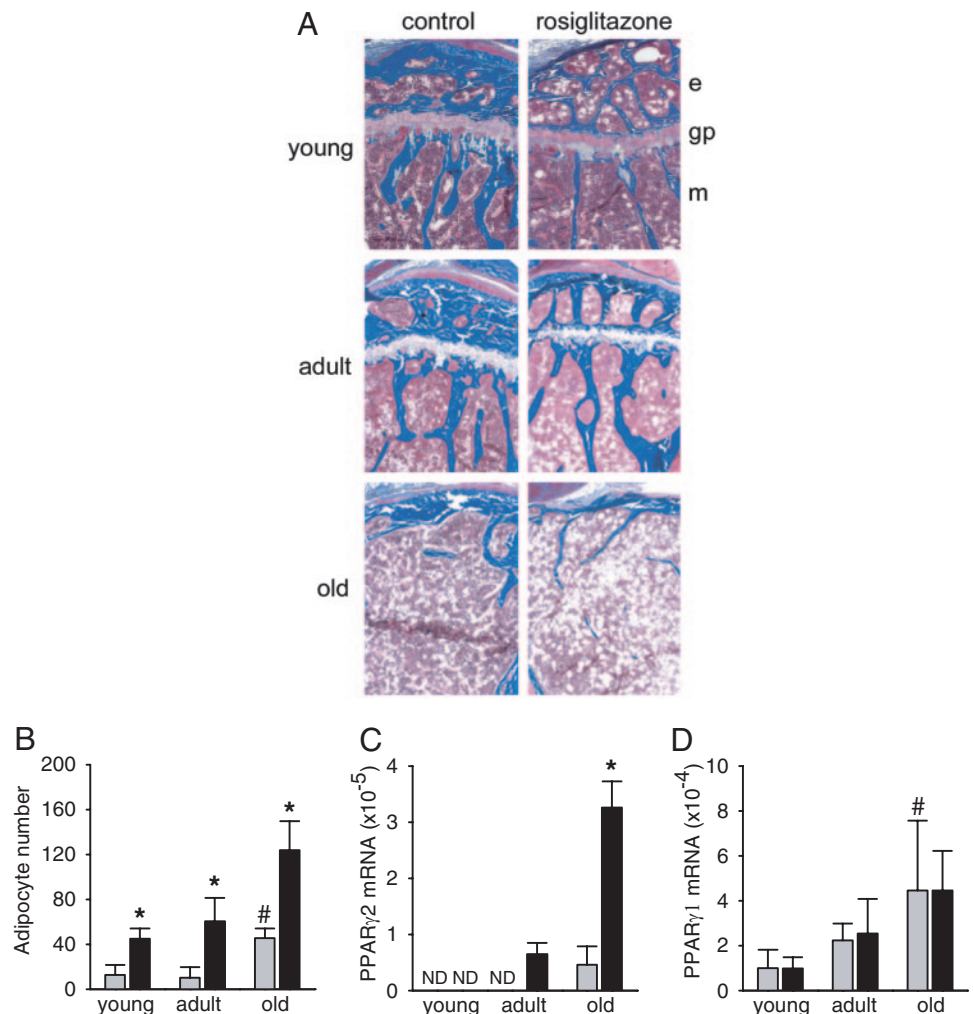


closely resembles the proximal tibia of aged animals (Fig. 7A). These similarities include the loss of bone in the epiphysis and fat accumulation in the marrow, which replaces bone. The loss of an intact epiphysis and an increase in adipocyte number is also seen in young animals treated with rosiglitazone (Fig. 7A). Because such changes in the epiphysis may affect longitudinal bone growth (28), we measured the length of the tibia in young animals using digital calipers. There were no significant differences in the length of the tibia in control vs. rosiglitazone-treated animals (data not shown).

The decrease in trabecular bone volume that occurs during

aging, and as a result of rosiglitazone treatment, is accompanied by an increase in the number of marrow adipocytes (Figs. 1 and 7, A and B). Rosiglitazone increased the number of marrow adipocytes regardless of the age of the animals. However, the largest increase was observed in old animals, which, even at the baseline, have higher numbers of marrow adipocytes. The increased number of adipocytes and the increased sensitivity of old marrow to the proadipocytic effect of rosiglitazone treatment can be attributed to the increased expression of the PPARγ2 isoform in MSC with aging (11).

FIG. 7. Examination of histological appearance and PPARγ expression in the proximal tibia. A, Histological appearance. Undecalcified tibiae were obtained from young, adult, and old control and rosiglitazone-treated mice and embedded in methyl methacrylate, sectioned, and stained with Golden trichrome (2). Mineralized bone tissue is stained blue. The unstained areas in the bone marrow represent empty spaces previously occupied by adipocytes. Magnification, ×4. e, Epiphysis; gp, growth plate; m, metaphysis. B, Marrow adipocyte number in the metaphysis of the proximal tibia. Adipocytes were recognized based on the distinct appearance of round empty spaces in the processed specimens. Cell numbers represent a mean of five fields per bone at magnification ×20. Data were collected from the tibiae of five animals from each group. C, Levels of PPARγ2 mRNA expression in whole tibia. D, Levels of PPARγ1 mRNA expression in whole tibia. Gene expression was measured using real-time PCR. Gray bars, control; black bars, rosiglitazone. *, *P* < 0.05 vs. control; #, *P* < 0.05 vs. young animals. ND, mRNA expression below detection level.



The number of adipocytes in the tibia of adult and old animals correlated with the increased expression of the adipocyte-specific PPAR γ 2 mRNA isoform (Fig. 7C). PPAR γ 2 was undetectable in the bones of young and adult control animals but was detected in the bone of old control animals. Rosiglitazone significantly increased PPAR γ 2 mRNA expression in the bone of adult and old, but not young, animals (Fig. 7C). In contrast, the expression of the more abundant and less specific PPAR γ 1 mRNA isoform was increased with aging but was not affected by rosiglitazone treatment (Fig. 7D). The differences in the pattern of expression of both PPAR γ isoforms may reflect their different cellular localization and/or distinct functions in the maintenance of skeletal homeostasis.

Rosiglitazone affects the multipotential phenotype of osteoblast progenitors

Analysis of the differentiation potential of the MSC compartment revealed that, in accordance with earlier reports (18), *in vivo* administration of rosiglitazone did not affect the potential of MSC to form fibroblast-like colonies, mineralized colonies (CFU-OB), or colonies of fat-laden cells (data not shown). These data suggest that the innate potential of MSC to acquire the osteoblastic or adipocytic phenotype is not affected by rosiglitazone. However, these measurements do not consider whether the multipotential character of bone marrow MSC, which changes with aging (37, 38), is affected by rosiglitazone treatment.

To assess the multipotential phenotype of MSC, experiments were designed based on the following rationale. We reasoned that the conversion of MSC between lineages is, at least in part, permitted in these cells by the simultaneous expression of both adipocytic (e.g. PPAR γ 2) and osteoblastic (e.g. Runx2) transcription factors. Previous evidence indicated that PPAR γ activation converts multipotential MSC to terminally differentiated adipocytes and irreversibly suppresses their osteoblast phenotype (10). Thus, rosiglitazone pretreatment of MSC, which are capable of differentiation down both lineages, will result in a reduction in the number of cells capable of osteoblastic differentiation. However, if the MSC have lost their bipotential phenotype, such pretreatment will not affect the number of osteoblastic progenitors.

As shown in Fig. 8A, the pretreatment of MSC derived from adult control animals with rosiglitazone for 3 d followed by stimulation toward osteoblastogenesis resulted in a significant decrease in the number of CFU-OB compared with control. This suggests that the pool of adult MSC contains a significant number of rosiglitazone-sensitive osteoblast progenitors, presumably because they express PPAR γ 2. In contrast, the same rosiglitazone pretreatment of MSC derived from adult rosiglitazone-treated animals did not significantly reduce the number of CFU-OB (Fig. 8A). Similarly, pretreatment of MSC derived from old animals, either control or rosiglitazone-treated, did not affect the number of CFU-OB (Fig. 8B). These data suggest that the osteoblastic progenitors derived from either rosiglitazone-treated adult or old animals are insensitive to rosiglitazone treatment *in vitro* and suggest that both exposure to rosiglitazone *in vivo*

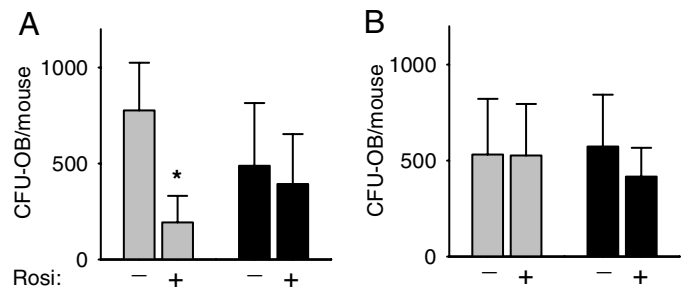


FIG. 8. Effect of aging and rosiglitazone treatment on osteoblastic MSC differentiation. Bone marrow cells derived from adult (8 months old) (A) and old (26 months old) (B) animals were either pretreated (+) or not (-) with rosiglitazone (10^{-6} M) for 3 d. The cells were then cultured in pro-osteoblastic medium for the next 28 d followed by von Kossa staining to visualize mineralized colonies. The number of von Kossa-stained CFU-OB was enumerated and calculated per total number of marrow cells isolated from two femora of an individual mouse. Cultures were established separately from individual animals. The following number of animals in each group was analyzed: adult, six control and four rosiglitazone; old, four control and six rosiglitazone. Gray bars, control; black bars, rosiglitazone-treated animals. *, $P < 0.05$ vs. no treatment.

and aging produce a similar loss of rosiglitazone responsiveness in the MSC compartment. Mechanistically, it is reasonable to presume that the *in vivo* exposure of multipotential MSC, which express PPAR γ 2 to rosiglitazone results in the terminal differentiation toward adipocytes and a simultaneous suppression of the osteoblast phenotype.

Discussion

We have previously postulated that an age-related increase in both the expression of the adipocyte-specific PPAR γ 2 isoform and levels of natural PPAR γ ligands, either locally produced in bone or delivered from the circulation, combined with a PPAR γ 2-mediated dominant negative effect on osteoblast phenotype, is a key mechanism in age-related bone loss (10, 11, 26). Here, we demonstrate that rosiglitazone induces skeletal changes, such as bone loss, closing of the epiphysis, marrow adiposity, and altered marrow MSC phenotype, which are reminiscent of the bone changes that occur with aging. Moreover, aging appears to be a confounding factor for rosiglitazone-induced bone loss.

Rosiglitazone-induced structural, morphological, and functional changes in the skeleton result in a decrease of both bone mass and bone strength, two important parameters of bone quality. At the cellular level, PPAR γ activation leads to changes in marrow structure and function, which are similar to the observed age-related changes and include a decrease in the number of osteoblasts, an increase in the number of marrow fat cells, and an increase in the number of osteoclasts. These changes are reflected at the molecular level by the decreased expression of osteoblast-specific and increased expression of adipocyte-specific gene markers (2, 11) and the increased expression of RANKL, the latter leading to increased osteoclastogenesis. Finally, rosiglitazone changes the multipotential character of MSC by decreasing their ability to interconvert between the osteoblastic and adipocytic lineages. In sum, rosiglitazone treatment *in vivo* modifies the phenotype of adult osteoblast progenitors to one that resem-

bles the phenotype of osteoblast progenitors derived from old animals (11, 37, 38).

The prevalence of type 2 diabetes is growing with an estimated 20 million prescriptions written annually (39). In recent years, the age of patients diagnosed with type 2 diabetes has progressively decreased, and the incidence of the disease among the very young has become even more common (40). In the animal model described here, rosiglitazone treatment induced significant bone loss in both adult and aged animals but not in young growing animals, although bone formation rate was significantly decreased. When considered together with the observed changes in the morphology of the epiphysis in young animals after rosiglitazone treatment, we expect that a longer duration of treatment or higher doses would induce significant bone loss, primarily as a result of the sustained suppression of bone formation rate. This observation is of particular importance because TZD therapies are increasingly being considered for younger patients.

Rosiglitazone-induced bone loss in adult and old animals appears to occur via distinct cellular mechanisms. Although bone loss in adult animals was associated with a decreased number of osteoblasts and decreased bone formation rate, the bone loss in old animals was a direct result of the increased osteoclast number. Based on the changes in the phenotype of bone marrow MSC, it is reasonable to conclude that in adult animals, rosiglitazone targets osteoblast progenitors and drives them to differentiate toward the adipocyte lineage. In contrast, rosiglitazone treatment of old animals does not appear to affect the differentiation of osteoblastic progenitors but instead alters MSC support for osteoclastogenesis. These possibilities are supported by data showing that the sensitivity of osteoblast progenitors to rosiglitazone decreases with aging. Consistent with this notion, in older animals, the increased adipocyte number after rosiglitazone treatment does not occur at the expense of osteoblast differentiation. In addition, because rosiglitazone increased the RANKL/OPG ratio as well as osteoclast number, bone loss in old animals is likely a result of increased bone resorption. When considered in the context of the rosiglitazone-mediated increases in osteoclastogenesis observed *in vivo*, these results suggest that rosiglitazone, like aging, increases the ability of MSC to support osteoclastogenesis. Interestingly, this effect correlates with the age-dependent increase in PPAR γ expression in the MSC compartment (11). In support of this idea, Sottile *et al.* (15) have suggested that rosiglitazone-induced bone loss in ovariectomized rats is due to increased bone resorption and not decreased bone formation. Based on the studies presented here, both age and bone formation rate are important factors in determining the mechanism of rosiglitazone-induced bone loss. If these data are confirmed in prospective clinical studies, it would argue strongly for the development of specific therapies, based on age and specific bone remodeling parameters, to prevent the bone loss associated with TZD therapy.

The role of PPAR γ in the regulation of osteoclast development is complex. It is well documented that TZD inhibit osteoclast differentiation and function through a direct action on cells of osteoclast lineage (34–36). Indeed, we have presented here that in *in vitro* conditions, a presence of ros-

iglitazone directly affects a process of osteoclast recruitment from the pool of hematopoietic progenitors. Interestingly, *in vivo* rosiglitazone had no effect on the number of osteoclasts in young and adult animals and increased osteoclast number in old animals. We and others suggest a role for PPAR γ in driving the increased ability of mesenchymal marrow cells to support osteoclast development. Schwab *et al.* (41) demonstrated previously that the PPAR γ agonist ciglitazone increased mesenchymal cell support for osteoclast development. Similarly, we demonstrated that osteoclast development was augmented by rosiglitazone via a mechanism involving an apparent synergistic effect of PPAR γ and vitamin D receptor on RANKL expression. Recently, two groups simultaneously reported the identification of a new enhancer region for RANKL gene, which determines its transcriptional regulation in response to the pro-osteoclastogenic hormones, vitamin D₃, and PTH (42, 43). It would be of particular interest to examine whether the crosstalk between the vitamin D receptor and PPAR γ 2 in the regulation of RANKL gene expression also involves this region. More studies are warranted investigating the *in vivo* effects of TZD on osteoclastogenesis and bone resorption.

During aging, the MSC compartment undergoes constant progressive changes, leading to the restricted differentiation potential of formerly multipotential cells (37, 38). These changes are considered a hallmark of the cellular senescence of marrow MSC. We have observed that both rosiglitazone and aging change the phenotype of MSC from multipotential to monopotential lineage-restricted cells. This alteration is manifested by a loss of the ability of osteoblastic cells to respond to rosiglitazone treatment, which may indicate the lack of or a decrease in PPAR γ expression. By analogy to the lineage allocation of hematopoietic stem cells, osteoblast and adipocyte differentiation likely occurs by a stochastic process, which is determined and limited by the presence of phenotype-specific transcription factors (44). Thus, osteoblast and adipocyte development is determined by Runx2 and PPAR γ 2, respectively, which are simultaneously expressed in multipotential MSC. A loss of one of these factors will render MSC resistant to stimuli driving differentiation down the associated lineage. If so, osteoblast-committed MSC from old animals represent a pool of cells that have lost their adipocytic potential, as determined by the absence of PPAR γ 2, and represent senescent osteoblast progenitors. This pool of cells is phenotypically distinct from the pool of osteoblastic progenitors resident in the adult marrow.

In support of the hypothesis of osteoblastic cellular senescence, it has been shown previously that the effect of rosiglitazone on osteoblast differentiation is dependent on the stage of their development (18). Thus, *ex vivo* treatment with rosiglitazone of early bone marrow cultures resulted in a decrease in osteoblast number and a suppression of osteoblast-specific gene markers, whereas treatment of late cultures did not affect osteoblast differentiation (18). By analogy, we consider adult MSC to represent the early cultures, which possess a fraction of the multipotential cells, and old MSC to represent late cultures, which primarily consist of lineage-committed cells. Thus, the loss of the multipotential

properties of adult MSC exposed to rosiglitazone *in vivo* is reminiscent of the effect of aging on these cells.

Changes in the status of MSC with aging result from both changes in the intrinsic differentiation potential and changes in the production of signaling molecules that contribute to the formation of a specific marrow microenvironment. Increases in the expression of PPAR γ and in the production of its natural activators (e.g. oxidized fatty acids) during aging suggest the increased activity of the receptor. Increased activity of PPAR γ (similar to aging) down-regulates the expression and activity of many regulatory pathways. We have demonstrated previously that aging and rosiglitazone down-regulate the activity of the TGF- β /bone morphogenetic protein signaling pathway (11, 45). Interestingly, this is not the only osteogenic pathway impacted. IGF-I signaling, a known regulator of skeletal homeostasis whose function decreases with aging, is also regulated by activation of PPAR γ (46). Indeed, rosiglitazone decreases the expression of both IGF-I and IGF-I receptor in marrow MSC and decreases the level of circulating IGF-I (46). These findings support the idea that rosiglitazone impacts skeletal metabolism via multiple mechanisms, which include a direct effect on MSC differentiation as well as endocrine and paracrine alterations of the marrow microenvironment.

In summary, rosiglitazone induces bone loss through its action on marrow mesenchymal cells and marrow microenvironment. The bone loss induced by rosiglitazone occurs via distinct mechanisms in both adult and aged mice. Our data suggest that these differences can be attributed to rosiglitazone effects on distinct cellular compartments. Aging and the level of PPAR γ expression are confounding factors for mediating rosiglitazone-induced bone loss. Further investigation of the link between bone and fat at the molecular and cellular level is warranted and may provide new insight into the understanding of diseases such as diabetes and osteoporosis and possibly enable the development of therapies effective for both.

Acknowledgments

We thank Nisreen S. Akel for DEXA scans and analysis.

Received November 28, 2006. Accepted February 16, 2007.

Address all correspondence and requests for reprints to: Beata Lecka-Czernik, Ph.D., Department of Geriatrics, Reynolds Institute on Aging, Slot 807, 629 Jack Stephens Drive, Little Rock, Arkansas 72205. E-mail: leckaczernikbeata@uams.edu.

This work was supported by National Institute on Aging Grant R01 AG1782 and American Diabetes Association Research Grant 1-03-RA-46 to B.L.-C. and the Carl L. Nelson Chair of Orthopaedic Surgery to L.J.S.

Present address for S.O.R.: Warsaw Medical Academy, Institute of Oncology, Warsaw, Poland.

Disclosure Summary: The authors have nothing to disclose.

References

1. U.S. Department of Health and Human Services 2004 Bone Health and Osteoporosis: a report of the Surgeon General. U.S. Department of Health and Human Services, Office of the Surgeon General, Rockville, MD
2. Rzonca SO, Suva LJ, Gaddy D, Montague DC, Lecka-Czernik B 2004 Bone is a target for the antidiabetic compound rosiglitazone. *Endocrinology* 145: 401–406
3. Akune T, Ohba S, Kamekura S, Yamaguchi M, Chung UI, Kubota N, Terachi Y, Harada Y, Azuma Y, Nakamura K, Kadowaki T, Kawaguchi H 2004 PPAR γ insufficiency enhances osteogenesis through osteoblast formation from bone marrow progenitors. *J Clin Invest* 113:846–855
4. Lehrke M, Lazar MA 2005 The many faces of PPAR γ . *Cell* 123:993–999
5. Rosen CJ, Bouxsein ML 2006 Mechanism of disease: is osteoporosis the obesity of bone? *Nat Clin Pract Rheumatol* 2:35–43
6. Manolagas SC 1998 Cellular and molecular mechanisms of osteoporosis. *Ageing* 10:182–190
7. Moore SG, Dawson KL 1990 Red and yellow marrow in the femur: age-related changes in appearance at MR imaging. *Radiology* 175:219–223
8. Jiang Y, Jahagirdar BN, Reinhardt RL, Schwartz RE, Keene CD, Ortiz-Gonzalez XR, Reyes M, Lenvik T, Lund T, Blackstad M, Du J, Aldrich S, Lisberg A, Low WC, Largaespada DA, Verfaillie CM 2002 Pluripotency of mesenchymal stem cells derived from adult marrow. *Nature* 418:41–49
9. Aubin JE 2001 Regulation of osteoblast formation and function. *Rev Endocr Metab Disord* 2:81–94
10. Lecka-Czernik B, Gubrij I, Moerman EA, Kajkenova O, Lipschitz DA, Manolagas SC, Jilka RL 1999 Inhibition of Osf2/Cbfa1 expression and terminal osteoblast differentiation by PPAR- γ 2. *J Cell Biochem* 74:357–371
11. Moerman EJ, Teng K, Lipschitz DA, Lecka-Czernik B 2004 Aging activates adipogenic and suppresses osteogenic programs in mesenchymal marrow stroma/stem cells: the role of PPAR- γ 2 transcription factor and TGF- β /BMP signaling pathways. *Ageing Cell* 3:379–389
12. Cao JJ, Wranski TJ, Iwaniec U, Phleger L, Kurimoto P, Boudignon B, Halloran BP 2005 Aging increases stromal/osteoblastic cell-induced osteoclastogenesis and alters the osteoclast precursor pool in the mouse. *J Bone Miner Res* 20:1659–1668
13. Ren D, Collingwood TN, Rebar EJ, Wolffe AP, Camp HS 2002 PPAR γ knockdown by engineered transcription factors: exogenous PPAR γ 2 but not PPAR γ 1 reactivates adipogenesis. *Genes Dev* 16:27–32
14. Willson TM, Lambert MH, Kliewer SA 2001 Peroxisome proliferator-activated receptor γ and metabolic disease. *Annu Rev Biochem* 70:341–367
15. Sottile V, Seuwen K, Kneissel M 2004 Enhanced marrow adipogenesis and bone resorption in estrogen-deprived rats treated with the PPAR γ agonist BRL49653 (rosiglitazone). *Calcif Tissue Int* 75:329–337
16. Soroceanu MA, Miao D, Bai XY, Su H, Goltzman D, Karaplis AC 2004 Rosiglitazone impacts negatively on bone by promoting osteoblast/osteocyte apoptosis. *J Endocrinol* 183:203–216
17. Cock TA, Back J, Eleftheriou F, Karsenty G, Kastner P, Chan S, Auwerx J 2004 Enhanced bone formation in lipodystrophic PPAR γ (hyp/hyp) mice relocates haematopoiesis to the spleen. *EMBO Rep* 5:1007–1012
18. Ali AA, Weinstein RS, Stewart SA, Parfitt AM, Manolagas SC, Jilka RL 2005 Rosiglitazone causes bone loss in mice by suppressing osteoblast differentiation and bone formation. *Endocrinology* 146:1226–1235
19. Schwartz AV, Sellmeyer DE, Vittinghoff E, Palermo L, Lecka-Czernik B, Feingold KR, Strotmeyer ES, Resnick HE, Carbone L, Beamer BA, Won Park S, Lane NE, Harris TB, Cummings SR 2006 Thiazolidinedione (TZD) use and bone loss in older diabetic adults. *J Clin Endocrinol Metab* 91:3349–3354
20. Ogawa S, Urano T, Hosoi T, Miyao M, Hoshino S, Fujita M, Shiraki M, Orimo H, Ouchi Y, Inoue S 1999 Association of bone mineral density with a polymorphism of the peroxisome proliferator-activated receptor γ gene: PPAR γ expression in osteoblasts. *Biochem Biophys Res Commun* 260:122–126
21. Kiel DP, Ferrari S, Cupples LA, Karasik D, Dupuis J, Rosen CJ, Imamovic A, Demissie S 2005 Polymorphism in the PPAR γ influence bone density in humans. *J Bone Miner Res* 20:S234
22. Lazarenko OP, Rzonca SO, Suva LJ, Lecka-Czernik B 2006 Netoglitazone is a PPAR- γ ligand with selective effects on bone and fat. *Bone* 38:74–85
23. Aronson J, Hogue WR, Flahiff CM, Gao GG, Shen XC, Skinner RA, Badger TM, Lumpkin CK, Jr 2001 Development of tensile strength during distraction osteogenesis in a rat model. *J Orthop Res* 19:64–69
24. Suva LJ, Seedor JG, Endo N, Quartuccio HA, Thompson DD, Bab I, Rodan GA 1993 Pattern of gene expression following rat tibial marrow ablation. *J Bone Miner Res* 8:379–388
25. Parfitt AM, Drezner MK, Glorieux FH, Kanis JA, Malluche H, Meunier PJ, Ott SM, Recker RR 1987 Bone histomorphometry: standardization of nomenclature, symbols, and units. Report of the ASBMR Histomorphometry Nomenclature Committee. *J Bone Miner Res* 2:595–610
26. Lecka-Czernik B, Moerman EJ, Grant DF, Lehmann JM, Manolagas SC, Jilka RL 2002 Divergent effects of selective peroxisome proliferator-activated receptor- γ 2 ligands on adipocyte *versus* osteoblast differentiation. *Endocrinology* 143:2376–2384
27. Halloran BP, Ferguson VL, Simske SJ, Burghardt A, Venton LL, Majumdar S 2002 Changes in bone structure and mass with advancing age in the male C57BL/6J mouse. *J Bone Miner Res* 17:1044–1050
28. Parfitt AM 1984 Age-related structural changes in trabecular and cortical bone: cellular mechanisms and biomechanical consequences. *Calcif Tissue Int* 36: S123–S128
29. Werner AL, Travaglini MT 2001 A review of rosiglitazone in type 2 diabetes mellitus. *Pharmacotherapy* 21:1082–1099
30. Theoleyre S, Wittrant Y, Tat SK, Fortun Y, Redini F, Heymann D 2004 The molecular triad OPG/RANK/RANKL: involvement in the orchestration of pathophysiological bone remodeling. *Cytokine Growth Factor Rev* 15:457–475
31. Teitelbaum SL, Ross FP 2003 Genetic regulation of osteoclast development and function. *Nat Rev Genet* 4:638–649

32. Asagiri M, Takayanagi H 2007 The molecular understanding of osteoclast differentiation. *Bone* 40:251–264
33. Teitelbaum SL, Tondravi MM, Ross FP 1997 Osteoclasts, macrophages, and the molecular mechanisms of bone resorption. *J Leukoc Biol* 61:381–388
34. Bendixen AC, Shevde NK, Dienger KM, Willson TM, Funk CD, Pike JW 2001 IL-4 inhibits osteoclast formation through a direct action on osteoclast precursors via peroxisome proliferator-activated receptor γ 1. *Proc Natl Acad Sci USA* 98:2443–2448
35. Okazaki R, Toriumi M, Fukumoto S, Miyamoto M, Fujita T, Tanaka K, Takeuchi Y 1999 Thiazolidinediones inhibit osteoclast-like cell formation and bone resorption *in vitro*. *Endocrinology* 140:5060–5065
36. Chan BY, Gartland A, Wilson PJ, Buckley KA, Dillon JP, Fraser WD, Gallagher JA 2007 PPAR agonists modulate human osteoclast formation and activity *in vitro*. *Bone* 40:149–159
37. Muraglia A, Cancedda R, Quarto R 2000 Clonal mesenchymal progenitors from human bone marrow differentiate *in vitro* according to a hierarchical model. *J Cell Sci* 113:1161–1166
38. Fehrer C, Lepperdinger G 2005 Mesenchymal stem cell aging. *Exp Gerontol* 40:926–930
39. Watts NB, D'Alessio DA 2006 Type 2 diabetes, thiazolidinediones: bad to the bone? *J Clin Endocrinol Metab* 91:3276–3278
40. Silverstein JH, Rosenbloom AL 2001 Type 2 diabetes in children. *Curr Diab Rep* 1:19–27
41. Schwab AM, Granholm S, Persson E, Wilkes B, Lerner UH, Conaway HH 2005 Stimulation of resorption in cultured mouse calvarial bones by thiazolidinediones. *Endocrinology* 146:4349–4361
42. Kim S, Yamazaki M, Zella LA, Shevde NK, Pike JW 2006 Activation of receptor activator of NF- κ B ligand gene expression by 1,25-dihydroxyvitamin D3 is mediated through multiple long-range enhancers. *Mol Cell Biol* 26:6469–6486
43. Fu Q, Manolagas SC, O'Brien CA 2006 Parathyroid hormone controls receptor activator of NF- κ B ligand gene expression via a distant transcriptional enhancer. *Mol Cell Biol* 26:6453–6468
44. Laslo P, Spooner CJ, Warmflash A, Lancki DW, Lee HJ, Sciammas R, Gantner BN, Dinner AR, Singh H 2006 Multilineage transcriptional priming and determination of alternate hematopoietic cell fates. *Cell* 126:755–766
45. Lecka-Czernik B, Teng K, Lazarenko OP 2004 Glitazones, the anti-diabetic PPAR- γ agonists, suppress osteoblast differentiation and the activity of TGF- β /BMP signaling pathways. *J Bone Miner Res* 19:SA171
46. Lecka-Czernik B, Ackert-Bicknell C, Adamo ML, Marmolejos V, Churchill GA, Shockley KR, Reid IR, Grey A, Rosen CJ 2007 Activation of peroxisome proliferator-activated receptor γ (PPAR γ) by rosiglitazone suppresses components of the insulin-like growth factor regulatory system *in vitro* and *in vivo*. *Endocrinology* 148:903–911

Endocrinology is published monthly by The Endocrine Society (<http://www.endo-society.org>), the foremost professional society serving the endocrine community.